Volume 56
Number 31
21 April 2020
Pages 4255–4370

ChemComm

Chemical Communications

rsc.li/chemcomm

ISSN 1359-7345

ROYAL SOCIETY OF CHEMISTRY

COMMUNICATION

Thien S. Nguyen and Cafer T. Yavuz

Quantifying the nitrogen effect on CO_2 capture using isoporous network polymers

ChemComm

ROYAL SOCIETY OF CHEMISTRY

COMMUNICATION

View Article Online
View Journal | View Issue

Cite this: *Chem. Commun.*, 2020, **56**, 4273

Received 7th February 2020,
Accepted 18th March 2020

DOI: 10.1039/d0cc00982b

rsc.li/chemcomm

Quantifying the nitrogen effect on CO_2 capture using isoporous network polymers†

Thien S. Nguyen[a] and Cafer T. Yavuz *[abc]

The impact of nitrogen atoms on CO_2 binding was evaluated for two isostructural porous bisimidazole-linked polymers (BILPs), which serendipitously had identical surface areas and pore size distributions, a very rare observation. The two structures differ only in the core of the trialdehyde component, the nitrogen atom (BILP-19) *versus* benzene ring (BILP-5). Such a slight difference, however, has brought about a stronger CO_2 capture capacity of BILP-19 and hence increased CO_2/N_2 separation capability.

Global climate change is closely associated with industrial emissions of greenhouse gases such as CO_2, CH_4, and N_2O.[1] Due to the increasing use of fossil fuels for manufacturing, transportation, and energy demands, carbon dioxide emission has become one of the major contributors to the climate change. A large portion of global CO_2 production is from the activity of fossil-fuel-based power plants. In these plants, CO_2 is generated during the combustion of the fuel with an abundant amount of oxygen. The resulting flue gas contains a high quantity of CO_2 along with N_2 as the major component. Therefore, an efficient strategy to prevent the increase of CO_2 presence in the atmosphere would be the post-combustion CO_2 capture technology, where an adsorbent, preferably porous, is employed to selectively confine CO_2 in the presence of the excessive N_2.[2–4] Many studies have shown that highly porous polymers with high surface areas and rich nitrogen contents showed great results for CO_2/N_2 separation purposes.[5–12] However, there has never been a study that either deliberately or serendipitously probes the influence of the nitrogen proportion on the CO_2 binding capability, with all other parameters kept unchanged. Here we show two structurally similar benzimidazole-linked polymers (BILPs) with exactly the same surface area and pore size distribution. The only difference is the nitrogen *versus* benzene core. CO_2 and N_2 uptake measurements were performed to evaluate the CO_2/N_2 selectivity of each material. As the data revealed, the nitrogen-cored polymer (BILP-19) showed 1.8–2.5 times higher CO_2/N_2 selectivity over the benzene-cored polymer (BILP-5). Q_{st} calculation was also carried out to gain more comprehension about the authentic governing factors of the CO_2 capturing power of the adsorbents.

BILPs were introduced by Hani El-Kaderi and his team.[5–7] But in this work we synthesized BILP-5 and BILP-19 using a method reported by the Cheon group[13] (Fig. 1) with slight modification from the corresponding trialdehyde and 1,2,4,5-benzenetetramine (BTA) (see the ESI† for detailed monomer synthesis). In a typical procedure, BTA was first dissolved in DMF at room temperature followed by the slow addition of the monomer aldehyde solution in DMF. The slow addition procedure would minimize the competing intermolecular imine formation for a more efficient intramolecular cyclization and hence secure the imidazole structure. After the addition was completed, water was then added dropwise and the mixture was heated to 80 °C and stirred at this temperature for 24 hours. The reactions were performed under open-flask conditions under which atmospheric oxygen would oxidize the dihydroxyimidazole rings to the imidazole products.

To gain structural insights into the obtained materials, a number of analytical characterization studies were carried out.

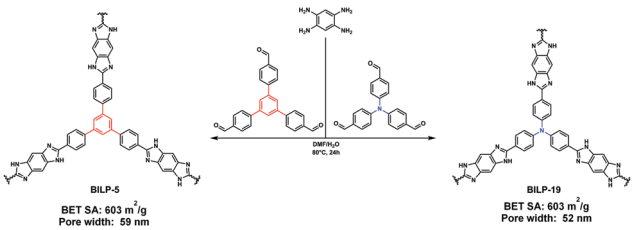

Fig. 1 The synthesis of bisimidazole polymers.

[a] *Graduate School of EEWS, Korea Advanced Institute of Science and Technology (KAIST), 291 Daehak-ro, Yuseong-gu, Daejeon 34141, Republic of Korea. E-mail: yavuz@kaist.ac.kr*
[b] *Department of Chemical and Biomolecular Engineering, KAIST, 291 Daehak-ro, Yuseong-gu, Daejeon 34141, Republic of Korea*
[c] *Department of Chemistry, KAIST, 291 Daehak-ro, Yuseong-gu, Daejeon 34141, Republic of Korea*

† Electronic supplementary information (ESI) available: Materials, synthetic methods, and NMR and BET characterization data. See DOI: 10.1039/d0cc00982b

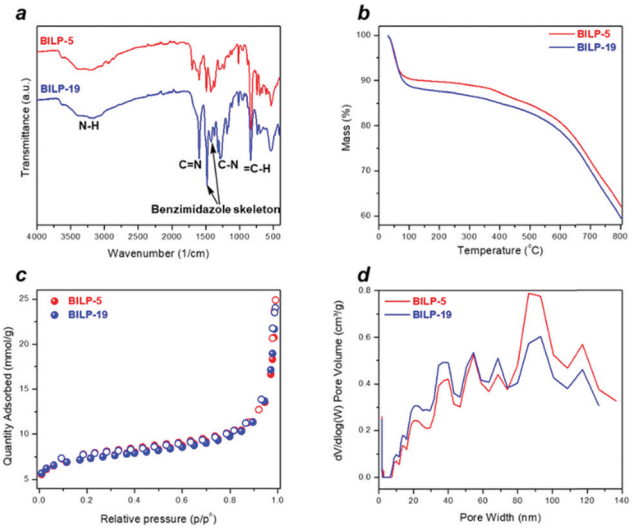

Fig. 2 Structural characterization of BILP-5 and BILP-19. (a) FT-IR spectra. (b) Thermogravimetric analysis. (c) Nitrogen adsorption–desorption isotherms at 77 K. (d) Pore size distribution.

The chemical functional identity and chemical connectivity of the polymers were confirmed by the FT-IR spectra and solid-state ^{13}C CP-MAS NMR. In the FT-IR spectra in Fig. 2a, the presence of benzimidazole N–H was represented by the signals at 3380 cm^{-1} and 3200 cm^{-1}. These peaks could be assigned to the free and hydrogen-bonded N–H stretching vibrations respectively. The characteristic C=N stretching signal appeared as an intense peak at 1598 cm^{-1} and benzimidazole skeleton vibrations were observed at 1495 cm^{-1} and 1420 cm^{-1}. Furthermore, the absence of aldehyde C=O stretching signals from the starting aldehydes was also observed, indicating the consumption of the monomer. The obtained IR spectra were compared against the reported spectra of the same materials and they showed a considerable resemblance.[14,15] The ^{13}C CP-MAS NMR spectra (Fig. S7, ESI†) featured the characteristic signal for imidazole carbon (C9 in BILP-5 and C7 in BILP-19) at ~150 ppm along with other aryl carbon peaks of the structure. A comparison with reported NMR spectra[14,15] to confirm the purity and identity of the materials was also done and significant similarity was observed. Thermogravimetric analysis (TGA) revealed identical thermal degradation profiles of the two polymers (Fig. 2b). The initial weight loss was recorded between 40 and 100 °C which resulted from the removal of residual solvents such as acetone and water. A major decomposition was recorded at about 400 °C in both materials. Such similar thermal stability portraits implied a uniform construct and porosity. Furthermore, scanning electron microscopy (SEM) images showed comparable surface morphologies of the polymers and revealed aggregated particles ~0.5–1.0 μm for both materials (Fig. S8, ESI†). Lastly, powder X-ray diffraction analysis (PXRD) confirmed the anticipation of the materials being amorphous (Fig. S9, ESI†).

Brunauer–Emmett–Teller (BET) calculation on the nitrogen adsorption–desorption isotherms at 77 K showed an unprecedented case of two structurally identical polymers having exactly equal surface areas. As shown in Fig. 2c, the isotherm curves completely overlapped to express the BET surface area of 603 m^2 g^{-1}. The non-linear density functional theory (NLDFT)-based pore size distribution yielded an average pore size of 59 nm for BILP-5 and a slightly smaller size of 52 nm for BILP-19, presumably due to the smaller size of the tris(4-formylphenyl)amine than 1,3,5-tris(4-formylphenyl)benzene monomer (Fig. 2d and Fig. S5, ESI†). These average pore sizes appeared to be much larger than previously reported values of the isostructural materials reported by the El-Kaderi group and others.[14,15] This could be due to the different synthetic approaches. In conventional methods, the network construction usually proceeds at low temperature (−30 °C to room temperature), and under such kinetically-controlled conditions, imine formation and cyclization happen with less reversibility and thus allow the aggregation to outcompete any reversible self-minimization of steric restriction. On the other hand, the BILPs in this study were accessed *via* a high temperature method, which to some extent facilitated a thermodynamic optimization to gain a sterically low energy arrangement through reversible processes. Regardless of this deviation from the common observation, this, to our knowledge, is at its unique value the first case where two structures with similar functionalities have similar morphologies.

The same surface area and pore size distribution have prompted an evaluation of their CO_2/N_2 separation capabilities. In particular, we aimed to examine the effect of a small structural difference of the nitrogen *versus* benzene core on the CO_2/N_2 selectivity taking advantage of the equal porosities of the materials. The CO_2 uptake isotherms of the polymers were obtained at three different temperatures. As shown in Fig. 3a, the materials produced almost similar CO_2 capturing profiles, and in all cases, BILP-19 appeared to have higher uptake values. The N_2 uptake, on the other hand, showed an inverse relationship where BILP-5 delivered higher uptake capacities (Fig. 3b). This

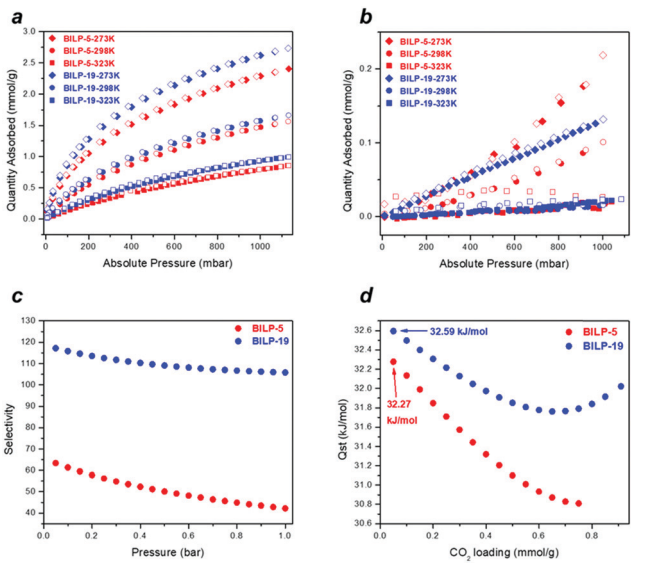

Fig. 3 Gas uptake properties of BILP-5 and BILP-19. (a) CO_2 adsorption–desorption isotherms at 273 K, 298 K and 323 K. (b) N_2 adsorption–desorption isotherms at 273 K, 298 K and 323 K. (c) CO_2/N_2 (15 : 85) selectivities at 298 K. (d) Isosteric heats of CO_2 adsorption.

could be accounted for by the enhanced π–π interaction with the N_2 molecule of BILP-5. This phenomenon was previously observed to facilitate N_2 uptake.[16] It is noteworthy that the CO_2 capture capacities obtained were all lower than previously reported values. This is also relatively unsurprising given the above-discussed large pore sizes, which endowed the studied materials with lower retention capacities or higher gas diffusion capability through the network.

In light of the above gas uptake behaviour, we turned to look into the gas selectivity for the CO_2/N_2 separation purpose. Using IAST calculations, we found that BILP-19 could, as expected, separate CO_2 from N_2 from 1.8 to 2.5 times more than BILP-5 in the pressure range of 0.05–1 bar with enhanced differences obtained at elevated pressures (Fig. 3c). This could possibly be due to the higher CO_2 binding of BILP-19 through greater interaction of the nitrogen atoms and CO_2. Furthermore, the contribution of the lower nitrogen uptake of BILP-19 to the superior selectivities of BILP-5 is critical. To examine how the CO_2 binding strength varies, the isosteric heats of CO_2 adsorption (Q_{st}) of the two materials were analysed. BILP-19, as predicted, showed higher values than BILP-5. However, in general, they were not dramatically different (Fig. 3d) or it could be stated that the distinction was negligible. This indicates that the addition of a nitrogen atom in BILP-19 did not increase significantly the binding strength but rather the captured amount of CO_2. It is hypothetically the conjugation of the lone pair to the benzene rings that restrains the nucleophilicity of the tertiary nitrogen and hence diminishes its chemisorptive interaction with the CO_2 carbon. At this point, the greater CO_2 capture ability of BILP-19 could be traced back to its smaller pore size that allowed a more efficient trapping effect and slightly more favourable binding to CO_2. Such significance of pore size in gas confinement, in particular CO_2, can also be found in the literature. An example is the case of chemically stable β-ketoenamine-linked covalent organic frameworks. TPPa-1,[17] the first of the class, with a BET surface area of 535 $m^2\ g^{-1}$ and pore sizes ranging from 0.8 to 1.5 ppm could capture CO_2 as much as 3.5 mmol g^{-1} (273 K, 1 bar), while its analogous structure, azoTP,[18,19] due to the longer azo-linkers had a larger pore size of 3.5 nm and hence exhibited a lower CO_2 uptake capacity of 2.4 mmol g^{-1} despite its much higher surface area (1552 $m^2\ g^{-1}$).

In summary, as a rare occasion, two isoporous, structurally similar bisimidazole polymers were serendipitously obtained. The slight difference in the core structure appeared to affect the CO_2 as well as N_2 capture ability. BILP-19, built on a nitrogen-centred trialdehyde, exhibited higher CO_2 uptake capacities but lower nitrogen capture capabilities than BILP-5, which was constructed on a benzene core. This, in turn, led to greater CO_2/N_2 selectivities for BILP-19. Q_{st} value determination revealed that the higher content of nitrogen in BILP-19 did not provide critically stronger binding to CO_2 carbons as demonstrated by almost equal Q_{st} values for the two polymers, and this was due to the lower nucleophilic nature of the conjugated nitrogens in BILP-19. The higher CO_2/N_2 separation potential of BILP-19 was indeed the combination of the higher retention of N_2 in the BILP-5 network through stronger π–π interaction and the minimal enhancement in CO_2 capture of BILP-19 owing to its smaller pore size. Above all, the uniform morphology and porosity of the studied materials have enabled these informative conclusions to be drawn.

This work was supported by National Research Foundation of Korea (NRF) grants funded by the Korean government (MSIP) (No. NRF-2017M3A7B4042140 and NRF-2017M3A7B4042235).

Conflicts of interest

There are no conflicts to declare.

Notes and references

1 F. H. M. Paul, *Absorption-Based Post-combustion Capture of Carbon Dioxide*, Woodhead Publishing, 2016.
2 H. A. Patel, J. Byun and C. T. Yavuz, *ChemSusChem*, 2017, **10**, 1303.
3 J. M. Huck, L. C. Lin, A. H. Berger, M. N. Shahrak, R. L. Martin, A. S. Bhown, M. Haranczyk, K. Reuter and B. Smit, *Energy Environ. Sci.*, 2014, **7**, 4132.
4 D. M. D'Alessandro, B. Smit and J. R. Long, *Angew. Chem., Int. Ed.*, 2010, **49**, 6058.
5 M. G. Rabbani, T. E. Reich, R. M. Kassab, K. T. Jackson and H. M. El-Kaderi, *Chem. Commun.*, 2012, **48**, 1141.
6 A. K. Sekizkardes, T. Islamoğlu, Z. Kahveci and H. M. El-Kaderi, *J. Mater. Chem. A*, 2014, **2**, 12492.
7 A. K. Sekizkardes, S. Altarawneh, Z. Kahveci, T. Islamotlu and H. M. El-Kaderi, *Macromolecules*, 2014, **47**, 8328.
8 T. M. McDonald, W. R. Lee, J. A. Mason, B. M. Wiers, C. S. Hong and J. R. Long, *J. Am. Chem. Soc.*, 2012, **134**, 7056.
9 G. Qi, L. Fu and E. P. Giannelis, *Nat. Commun.*, 2014, **5**, 1.
10 H. A. Patel, S. Hyun Je, J. Park, D. P. Chen, Y. Jung, C. T. Yavuz and A. Coskun, *Nat. Commun.*, 2013, **4**, 1357.
11 J. Byun, D. Thirion and C. T. Yavuz, *Beilstein J. Nanotechnol.*, 2019, **10**, 1844.
12 S. Subramanian, J. Oppenheim, D. Kim, T. S. Nguyen, W. M. H. Silo, B. Kim, W. A. Goddard and C. T. Yavuz, *Chem*, 2019, **5**, 3232.
13 Y. S. Lee, Y. H. Cho, S. Lee, J. K. Bin, J. Yang, G. Chae and C. H. Cheon, *Tetrahedron*, 2015, **71**, 532.
14 M. G. Rabbani and H. M. El-Kaderi, *Chem. Mater.*, 2012, **24**, 1511.
15 C. Klumpen, F. Radakovitsch, A. Jess and J. R. Senker, *Molecules*, 2017, **22**, 1343.
16 P. Ray, D. Gidley, J. V. Badding and A. D. Lueking, *Microporous Mesoporous Mater.*, 2019, **277**, 29.
17 S. Kandambeth, A. Mallick, B. Lukose, M. V. Mane, T. Heine and R. Banerjee, *J. Am. Chem. Soc.*, 2012, **134**, 19524.
18 S. Chandra, T. Kundu, S. Kandambeth, R. Babarao, Y. Marathe, S. M. Kunjir and R. Banerjee, *J. Am. Chem. Soc.*, 2014, **136**, 6570.
19 R. Ge, D. Hao, Q. Shi, B. Dong, W. Leng, C. Wang and Y. Gao, *J. Chem. Eng. Data*, 2016, **61**, 1904.